Geophysical Research Letters

RESEARCH LETTER
10.1029/2022GL099133

Irminger Sea Is the Center of Action for Subpolar AMOC Variability

L. Chafik[1], N. P. Holliday[1], S. Bacon[1], and T. Rossby[2]

[1]National Oceanography Centre, Southampton, UK, [2]Graduate School of Oceanography, University of Rhode Island, Kingston, RI, USA

Key Points:

- Irminger Sea is the center of action for subpolar Atlantic Meridional Overturning Circulation (AMOC) variability from interannual to multidecadal time scales
- Irminger Sea density variations are controlled by the North Atlantic Oscillation through its subpolar gyre connection to the Labrador Sea
- Irminger Sea density trends suggests uncertain weakening of the subpolar AMOC since 1950

Supporting Information:

Supporting Information may be found in the online version of this article.

Correspondence to:

L. Chafik,
leon.chafik@noc.ac.uk

Citation:

Chafik, L., Holliday, N. P., Bacon, S., & Rossby, T. (2022). Irminger Sea is the center of action for subpolar AMOC variability. *Geophysical Research Letters*, *49*, e2022GL099133. https://doi.org/10.1029/2022GL099133

Received 12 APR 2022
Accepted 25 AUG 2022

Abstract Significant societally important climate impacts can be caused by changes in the strength of the Atlantic Meridional Overturning Circulation (AMOC) at higher latitudes. Focusing on variability and long-term change of the subpolar North Atlantic (SPNA)—a key AMOC action center—and using eastern OSNAP array observations, we identify a distinct density and sea-surface height signature of the AMOC strength in the Irminger Sea (2014–2018), reinforced and extended with an ocean reanalysis (1993–2018). Reconstruction of AMOC variability using Irminger Sea density shows strong control by the North Atlantic Oscillation on subpolar overturning on multiple timescales, achieved via the gyre circulation and waters from the Labrador Sea. Furthermore, the observed decrease of Irminger Sea density since the mid-twentieth century (1950–2019) is suggestive of a long-term AMOC weakening of 2.2 Sv or 13%, however, this trend remains statistically insignificant due to the large interannual and decadal variability of the SPNA.

Plain Language Summary The subpolar North Atlantic (SPNA) Ocean between Greenland and Scotland is a region that is key to the health of the Gulf Stream system. Here, the warm currents carrying heat from the subtropics become denser along their way from Scotland toward Greenland; a process that has a strong imprint on the strength of this vital ocean current system. In this work, we find that ocean density in the Irminger Sea east of Greenland in the SPNA explains most of the variability of the directly measured strength of the Gulf Stream system. Based on this relationship, we reconstruct density variations in this region from historical hydrographic observations to reveal whether the Gulf Stream system in the SPNA has been changing over the past 70 years. While there is suggestive evidence for a slow-down of this system in the SPNA in recent decades there is no consensus regarding its relevance to longer timescales.

1. Introduction

The climate-regulating meridional overturning circulation in the Atlantic Ocean is largely hidden from us (Lozier, 2012) and although continuous monitoring of its strength only commenced in 2004 and 2014 in the subtropical (Frajka-Williams, 2015) and subpolar (Lozier et al., 2017) North Atlantic, respectively, this rich system of ocean currents conveying heat and freshwater to higher latitudes is claimed, largely based on sea-surface temperature proxies, to have slowed down during the twentieth century (e.g., Caesar et al., 2018). Some studies have, however, pointed out that serious care should be taken when interpreting and attributing North Atlantic sea-surface temperature change to Atlantic Meridional Overturning Circulation (AMOC) slowdown since atmospheric effects play a large role in establishing these trends and, as such, these proxies are poor predictors of AMOC strength (Little et al., 2020; Hu & Fedorov, 2020; Keil et al., 2020; L. Li et al., 2022). The recent IPCC sixth assessment report further concluded that our confidence in both reconstructed and modeled AMOC changes is low and uncertain since it is still poorly constrained.

Another complication is that, on decadal timescales, the overturning variability appears to differ in the North Atlantic between subtropical and subpolar latitudes (see Jackson et al., 2022, and references therein). Because of the lack of decadal-scale coherency between these two regions, it is indeed uncertain which aspect of the AMOC available large-scale proxies represent. As an example, the widely used reconstruction of the AMOC index based on sea-surface temperatures by Caesar et al. (2018) shows a strong decadal covariability and similar trend as the AMOC estimate from the RAPID array in the subtropical North Atlantic (see their Figure 6). Thus, our understanding of how the overturning circulation has evolved in the wider North Atlantic cannot be deduced from a single metric, and especially if not based on direct AMOC estimates in the first place.

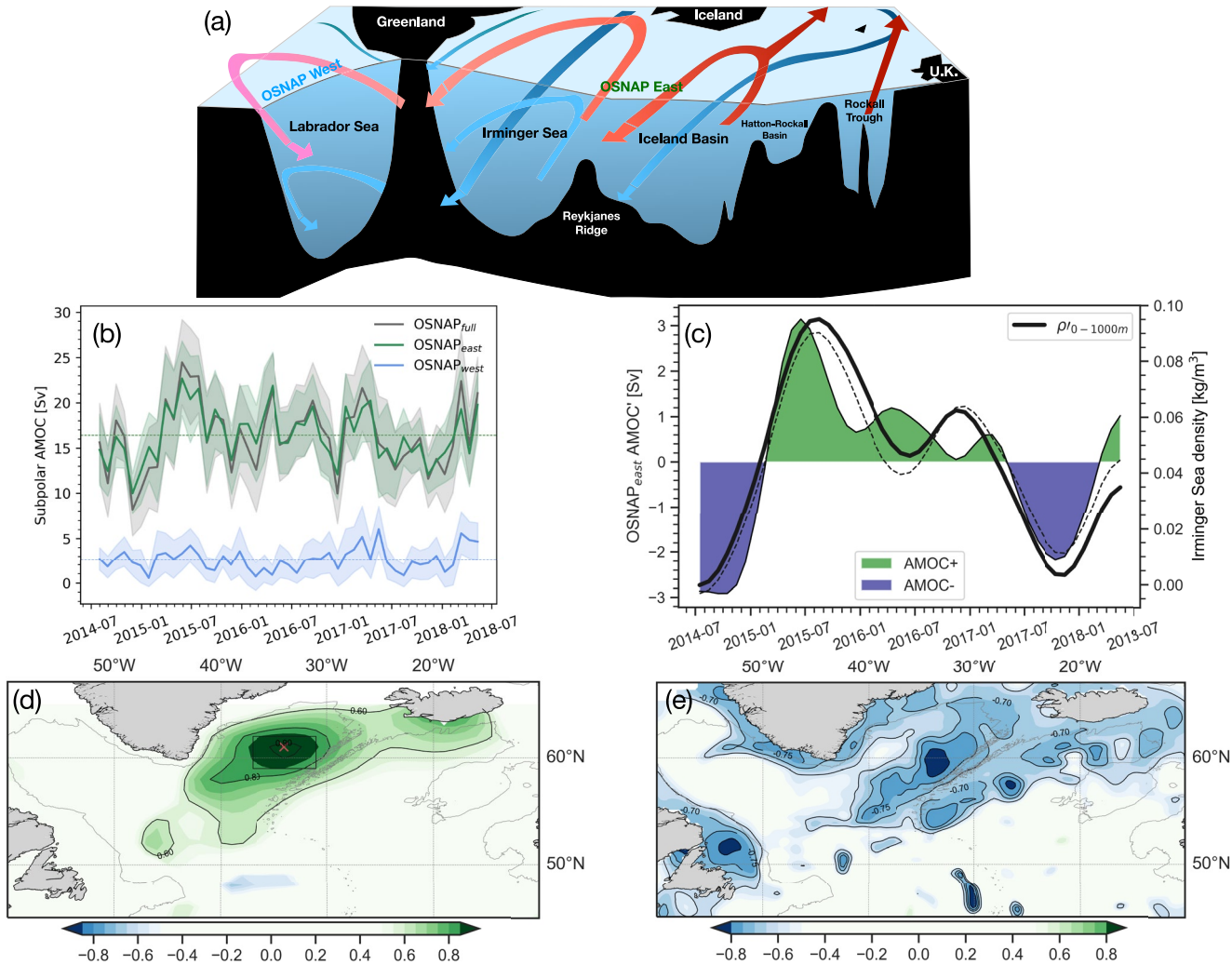

Figure 1. Subpolar overturning linkages from OSNAP. (a) The OSNAP East and West sections overlaid by the warm surface currents (red and pink) and the cold deep currents (blue). (b) Atlantic Meridional Overturning Circulation (AMOC) time series (Sv) across the full OSNAP array (light gray), OSNAP west (blue), and OSNAP East (green). The uncertainty using a 30-day Monte Carlo method is represented by the shading (F. Li et al., 2021). (c) AMOC anomaly (time-mean removed) at OSNAP East between 2014 and 2018 (shading). The solid black line is the 0–1,000 m averaged density in the Irminger Sea (see black box [31°–37°W and 59°–62°N], in panel d). The dashed black line represents the same as the solid line but for the location of maximum correlation (cf. red cross in panel d). Both time series have been filtered with a 12-month Butterworth filter. (d) Spatial correlation pattern between upper-ocean density (0–1,000 m) and AMOC time series at OSNAP East using the same filter as in panel b. (e) Same as panel (d) but for sea-surface heights. The thin gray contour in the lower panels is the 1,500 m isobath.

In the present study, we examine, for the first time, the signature of the overturning in the subpolar North Atlantic (SPNA) that is rooted in direct AMOC estimates. The objectives of this study are thus to reveal the signature of subpolar AMOC variability at its dominant source between Greenland and Scotland (Chafik & Rossby, 2019; Lozier et al., 2019) from direct AMOC observations at the OSNAP East array on interannual timescales (2014–2018; Figure 1a), assess the robustness of this signature on decadal timescales using an ocean reanalysis (1993–2019) to gain confidence when developing an indicator of long-term overturning changes, and shed some light on the underlying physical mechanisms.

Our observational results show evidence that strong subpolar overturning periods coincide with colder and denser upper-ocean water mass conditions, especially in the subpolar Irminger Sea. This observed pattern, which is supported by an ocean reanalysis over a longer period than OSNAP, indeed challenges the expected paradigm that decadal-long cooling in the SPNA are associated with a weakening decadal AMOC commonly painted by sea-surface temperature proxies mentioned above. Furthermore, the observed subpolar AMOC fingerprint developed here is suggestive of a long-term weakening, although this trend is still statistically insignificant due to the

large interannual and decadal variability in the SPNA. Before reaching this conclusion, however, we examine the underlying mechanisms of subpolar AMOC variability. A surprising finding is that density changes in the subpolar Irminger Sea, which explains most of the variability of the overturning between Greenland and Scotland, do not coincide with the region of the largest heat losses that are instead found in the Labrador Sea. We propose that the waters reaching the Irminger Sea are cooled in the first place in the Labrador Sea as a result of strong North Atlantic Oscillation (NAO) periods before being advected eastwards by the subpolar gyre circulation. This linkage is demonstrated using a backward Lagrangian tracking method applied to satellite altimetry and suggests that although the Labrador Sea does not dominate the subpolar overturning, it may play a key role in preconditioning the waters that facilitate the overturning process in the eastern subpolar gyre.

2. Data and Methods

2.1. OSNAP AMOC Time Series

We use the maximum transport of the overturning stream function as observed at OSNAP (Lozier et al., 2019; F. Li et al., 2021). We will, however, focus our study to the AMOC as measured at the eastern part of the OSNAP array, the section between Greenland and Scotland, since this dominates the mean overturning and its variability (Chafik & Rossby, 2019; Lozier et al., 2019; Zhang & Thomas, 2021). The time series used here are based on calculations of the overturning stream function in density space (σ_θ):

$$AMOC(t) = \max[\Psi(\sigma, t)] = \max\left[\int_{surface}^{\sigma}\int_{x_w}^{x_e} v(x,\sigma,t)dxd\sigma\right]\left(Sv741 = 10^6 \mathrm{m}^3\mathrm{s}^{-1}\right) \quad (1)$$

where the volume transport, v, which is perpendicular to the OSNAP East section is integrated zonally, x, from the western boundary, x_w, to the eastern boundary, x_e, and then integrated vertically from the surface across density layers, σ. The AMOC in density space is essentially measuring the transformation of water and is especially important for subpolar and higher latitudes where isopycnals are strongly tilted.

2.2. Hydrography and Sea-Surface Heights

For the hydrography, we use the quality controlled and objectively analyzed data of the Met Office, version EN4.2.1 (Good et al., 2013) covering the 1950–2019 period. From this gridded data set, we calculate the ocean density from the temperature and salinity fields and average in the upper 1000 m. We also use the monthly sea-surface heights derived from satellite altimetry. This data set was retrieved as daily fields from the Copernicus Marine Service (CMEMS). For the spatial correlation patterns based on the AMOC OSNAP East time series, the 2014–2018 ocean density and sea-surface height time-mean was removed from the data before a fourth-order Butterworth filter with a cut-off window of 12 months was applied to smooth the data on interannual timescales.

2.3. GloSea5 Ocean Reanalysis

We use the monthly fields (1993–2019) of global ocean and sea-ice reanalysis GloSea5 (Blockley et al., 2014; Jackson et al., 2016), namely FOAM-GloSea5v13, which uses the NEMO3.4 model with a nominal resolution of 0.25° (ORCA1/4°) and 75 vertical levels. The ocean reanalysis is available through CMEMS. We use the subpolar overturning time series from the reanalysis calculated in a similar fashion as described above for the eastern part of the OSNAP array using the original model grid. The GloSea5 AMOC time series, both in the subtropics and the SPNA, have been shown to compare well with the observations (Jackson et al., 2022). We also use sea-surface heights and temperature/salinity fields to calculate ocean density.

2.4. Atmospheric Reanalyses

We use the NCEP/NCAR reanalysis (Kalnay et al., 1996) to calculate the wind stress curl and the surface net heat flux. To calculate the wind stress curl, we use the monthly zonal and meridional wind stress components over the 1950–2019 period. We then calculate the first leading Empirical Orthogonal Function (EOF; Dawson, 2016) mode and associated principal component of wind-stress curl variability from these monthly fields. The spatial pattern of this first EOF mode mainly reflects the NAO—the leading mode of atmospheric variability over

the North Atlantic sector—that is signified by positive and negative wind-stress curl south of Iceland (i.e., the Icelandic low) and in the subtropics close to the Azores (i.e., the Azores high), respectively. The wind-stress curl fields have been linearly detrended and deseasonalized prior to the analysis. Because of the importance of the wind-stress curl for the basin-scale ocean circulation, we choose this variable over the mean sea-level pressure to capture the leading EOF mode of atmospheric variability. To calculate the surface net heat flux, we sum over the following monthly mean flux components: shortwave radiation, longwave radiation, sensible heat flux, and latent heat flux. Negative surface net heat flux means heat loss from the ocean to the atmosphere.

3. Results

3.1. Irminger Sea as a Center of Action for Subpolar AMOC Variability From OSNAP

First, we examine whether the OSNAP time series of subpolar AMOC has statistically significant relationships with dynamic indicators (sea surface height and density of the upper 1 km of the ocean). On interannual timescales the AMOC anomaly at OSNAP East shows a pattern of positive anomaly during the 2015–2016 period and a negative anomaly in 2014 and 2017 (Figure 1c). We find that a strengthening (weakening) of the subpolar AMOC anomaly coincides with anomalous increase (decrease) in upper-ocean density (0–1,000 m), especially in the Irminger Sea west of the Reykjanes Ridge (Figures 1c and 1d). Furthermore, as a result of anomalous subpolar AMOC increase, a coherent depressed dynamic height spatial pattern (Figure 1e) is seen to dominate the eastern SPNA with the largest changes in the Irminger Sea. The dynamic height pattern reflects the spatial density pattern (Figure 1d), and reveals that increased subpolar AMOC on interannual timescales is strongly associated with increased 0–1,000 m densities and decreased sea-surface heights in the Irminger Sea. This is the first time that this strong relationship has been observed with direct subpolar AMOC observations.

The density structure in the Irminger Sea is revealing of a pronounced shoaling of the 27.55–27.7 isopycnals, that is, the AMOC maxima at OSNAP East (see Figure S1 in Supporting Information S1), west of the Reykjanes Ridge during AMOC+ as compared to AMOC− periods (Figure 1b). As a consequence, there is a relationship between subpolar AMOC anomaly at the eastern part of the OSNAP array and density variability in the Irminger Sea away from the western boundary current east of Greenland, on interannual timescales. This suggests that satellite-derived sea-surface heights over the altimetry period or density anomalies in the Irminger Sea from hydrography may be useful predictors or proxies of interannual-to-decadal and long-term subpolar AMOC changes, as demonstrated in the next sections.

3.2. Irminger Sea as a Center of Action for Subpolar AMOC Variability From GloSea5

Since the subpolar AMOC time series from the eastern part of the OSNAP array only span the 2014–2018 period, we turn to an ocean reanalysis to confirm the robustness of the observed sea-surface height and upper-ocean density patterns. The GloSea5 ocean reanalysis is used for this purpose since its AMOC variability has been shown to be comparable to observations from both the RAPID and OSNAP arrays (Jackson et al., 2022; Moat et al., 2020; Zou et al., 2020).

We find the same significant relationship between the strength of subpolar AMOC and sea surface height over the past three decades. The subpolar AMOC variability in density space from GloSea5 shows a clear decadal variability with anomalously positive periods before mid-1990s and after 2010 and anomalously negative periods centered around 2000s. (The GloSea5 and OSNAP East AMOC are well correlated, $R = 0.73$, during the 2014–2018 period, and their standard deviations on interannual timescales are comparable, 1.6 vs. 1.82 Sv.) The subpolar AMOC is found to correlate well ($R = 0.84$) with the leading principal component of sea-surface height variability in the SPNA from both GloSea5 and satellite altimetry (Figure 2a; note, however, that the compatibility between the sea-surface height principal components is not surprising since GloSea5 assimilates satellite altimetry). The regression analysis of sea-surface heights onto the subpolar AMOC variability (Figure 2c) and the leading principal component of sea-surface height variability (Figure 2d) demonstrate nearly identical patterns. Both show a center of action in the Irminger Sea, that is, in the same location as the upper-ocean density regression pattern (Figure 2b). Despite the slight geographical difference as compared to observations (Figure 1 and Figure S2 in Supporting Information S1 showing the correlation pattern based on GloSea5), the subpolar Irminger Sea once again stands out as a hot-spot for AMOC variability in the eastern subpolar gyre as it explains

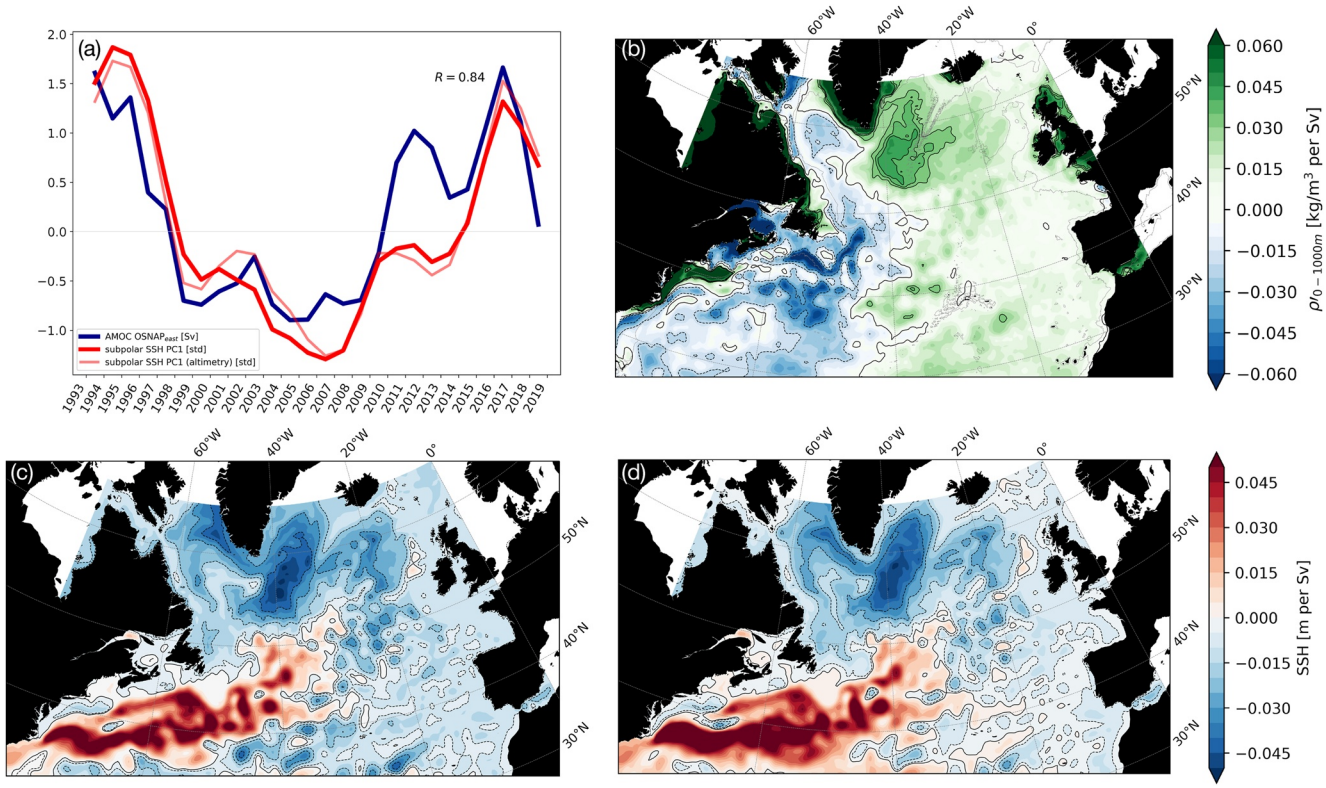

Figure 2. Subpolar overturning linkages from GloSea5. (a) Atlantic Meridional Overturning Circulation (AMOC) anomaly time series (1993–2019; Sv) at OSNAP East from GloSea5 (blue), and the leading principal component of sea-surface height (SSH) variability in the subpolar North Atlantic from GloSea5 (red) and altimetry (light red). The SSH principal components have been standardized (std). The GloSea5 leading EOF mode of SSH variability explains 31.4% of the variance. (b) Regression pattern of upper-ocean density (0–1,000 m) onto the subpolar AMOC at OSNAP East. The thin gray contour represents the 1,500 m isobath. (c) Same as (b) but using sea-surface heights. (d) Same as (c) but the regression pattern is now based on the leading principal component of SSH variability (red curve in panel a). To represent interannual-to-decadal variability, a 3-year running mean has been applied before the analyses.

a large fraction of the variance, consistent with the observed patterns from OSNAP (Figure 1) and despite the shortness of the time series.

The satellite-derived sea-surface heights since 1993 or upper-ocean density variations from historical hydrographic observations can thus be used with confidence to reconstruct and diagnose AMOC variability in the eastern SPNA, where both the mean and the variability of the overturning strength dominates. It is important to note, however, that neither sea-surface heights nor upper-ocean density are revealing of any mechanisms involved in generating these subpolar AMOC variations.

3.3. Atmosphere-Ocean Linkages of Subpolar AMOC Variability: A Role for the Labrador Sea and Gyre Circulation

In this section, we investigate the origin of the Irminger Sea upper-ocean density. In particular, we want to identify the roles of local atmospheric forcing, far-field atmospheric forcing, and ocean circulation. Our motivation is the apparent disconnect in location of the density anomalies that determine the strength of the subpolar AMOC in the Irminger Sea, and the locality of the maximum buoyancy loss due to cold winter winds in the Labrador Sea (Figure 3).

Numerous modeling studies have suggested that the NAO is a key mechanism that induces AMOC changes via anomalous surface heat flux in the Labrador Sea that influences the rate of North Atlantic Deep Water formation (see, e.g., Zhang et al., 2019, and references therein). The mechanism invoked is as follows: strong NAO associated with stronger westerly winds leads to enhanced surface heat loss and stronger dense water formation over the Labrador Sea, which, in turn, strengthens the overturning. This view that the Labrador Sea shapes the evolution

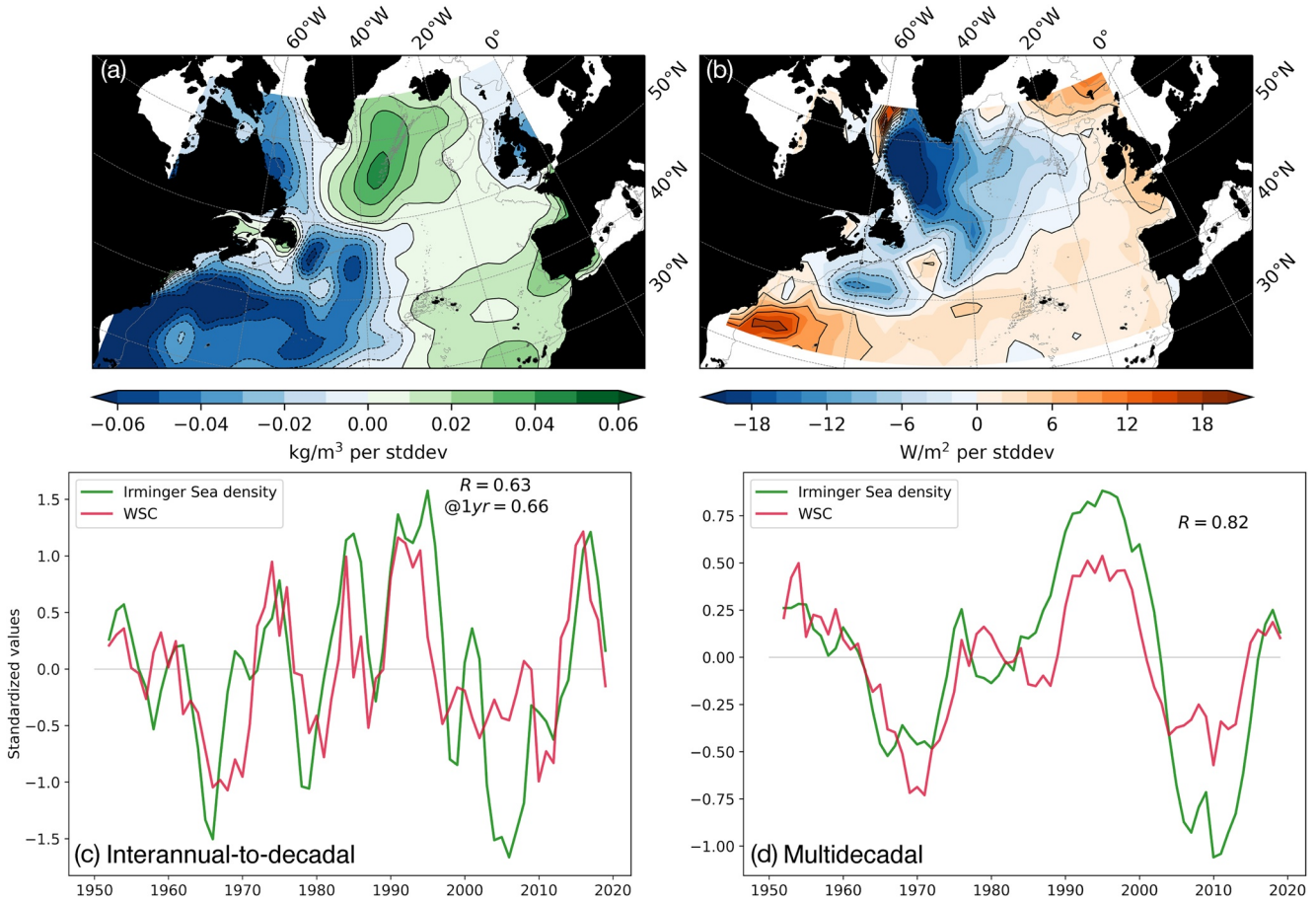

Figure 3. Large-scale pattern associated with Irminger Sea density variations. (a) Regression pattern of upper-ocean density variations (0–1,000 m) onto the leading principal component of wind-stress curl (WSC) variability. (b) Same as panel (a) but for net heat flux variations. (c) Irminger Sea density (averaged in a similar box as in Figure 1c) and the leading principal component of WSC variability smoothed using a 3-year running mean to highlight the interannual-to-decadal variability. The correlation coefficient, *R*, is shown within the figure. The WSC variability leads Irminger Sea density by 1 year (maximum lag correlation) as indicated in panel a (at lead in number of years) and assessed using cross-correlation analysis. The thin gray contour in the upper panels represents the 1,500 m isobath. (d) Same as panel (c) but on multi-decadal time scales (10-year running mean).

of the AMOC was, however, challenged recently by the OSNAP estimates (Lozier et al., 2019) and shown to be model-dependent (F. Li et al., 2019). Subsequently, Menary et al. (2020) showed that model density anomalies in the Labrador Sea in fact originated in the Irminger Sea and Iceland Basin, thus suggesting that the new observations do not necessarily contradict all earlier modeling studies.

However, the cyclonic circulation of the subpolar gyre acts to retain mode waters in the central region, as indicated by closed dynamic height contours (e.g., Foukal and Lozier, 2017). The strength of the gyre circulation is sensitive to the zonal dynamic height gradient and has been shown to increase when heat loss is high in the Labrador Sea (Häkkinen & Rhines, 2004). The gyre circulation is also sensitive to wind stress curl, and changes in the atmospheric circulation pattern can additionally determine the pathways of colder or warmer waters in the subpolar region (Desbruyères et al., 2021; Häkkinen et al., 2011; Holliday et al., 2020). This essentially means that effects of buoyancy loss in the Labrador Sea have the potential to subsequently impact Irminger Sea upper ocean density via the subpolar gyre circulation.

Here, we examine the relationship between the atmospheric circulation and the generation of Irminger Sea upper-ocean density anomalies by focusing on the wind stress curl. Figure 3 shows that the leading principal component of wind-stress curl variability (NAO-like) projects onto a large-scale horse-shoe pattern of positive density anomalies with a maximum loading over the eastern SPNA extending to the subtropics through the eastern side of the basin, and negative density anomalies along the Gulf Stream path and its extension.

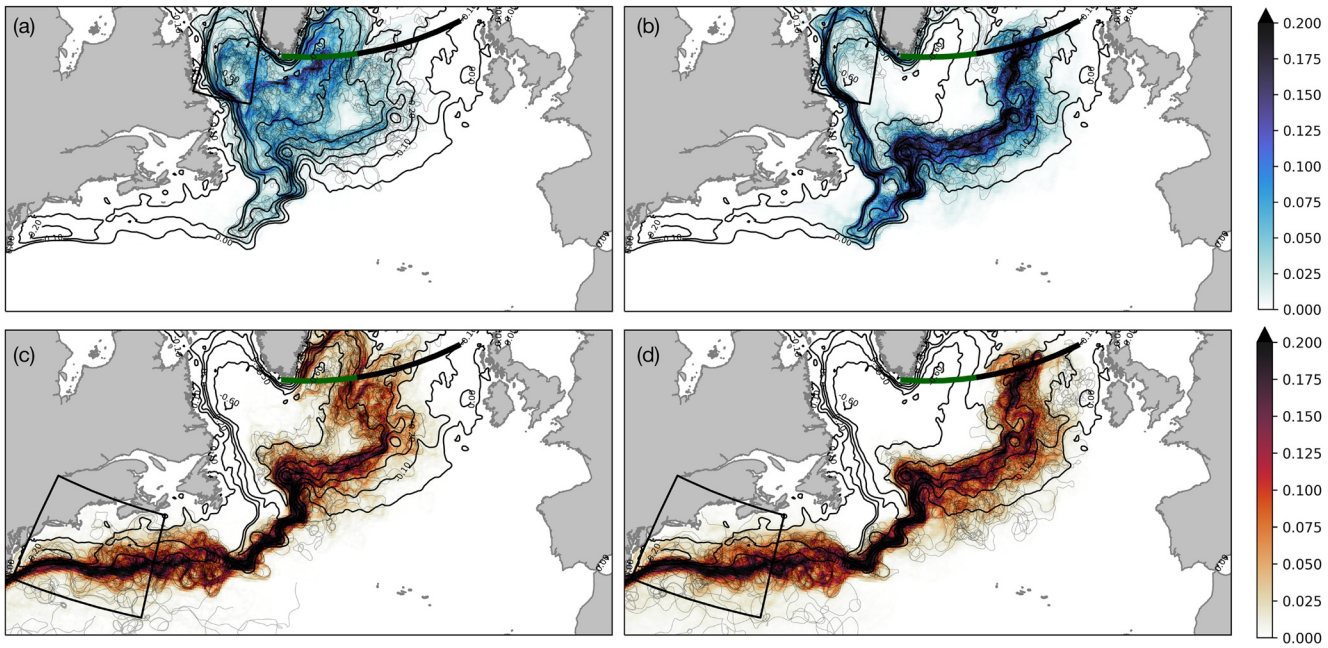

Figure 4. The dominant role of the Labrador Sea in filling the Irminger Sea. Lagrangian particle back-tracking to determine pathways of water based on a set of 4-year long trajectories initialized in the year 2016. The particles are released from (a) the Irminger Sea (thick green line from Greenland to the Reykjanes Ridge) and (b) the Iceland Basin (thick black from Reykjanes Ridge to the Hatton-Rockall Basin) to the Labrador Sea (see black box in upper panels). (c and d) are the same as (a and b) but particles are backtracked to the subtropics in the Gulf Stream region (see black box in lower panels). The shading shows the fraction of the particles that passed through each grid box. The bin size is 0.25° × 0.25°. The density maps are overlaid by 50 random particles (thin black lines). The black contours show mean absolute dynamic topography (Mulet et al., 2021). The Lagrangian analysis was performed with the TRACMASS tool using satellite-derived geostrophic velocity fields (Döös et al., 2017).

This pattern, which most importantly includes a center of action over the Irminger Sea, is reminiscent of that produced by GloSea5 (Figure 2b). This NAO-like variability is found to explain 40% (67%) of the observed Irminger Sea density variability on interannual-to-decadal (multidecadal) timescales, Figure 3c,3d, which reinforces the robustness of this atmospheric mechanism in impacting the overturning strength in the eastern SPNA (the NAO-like and the Irminger Sea density variations produce nearly identical regression patterns in the SPNA). There exists, however, an asymmetry between the regions of greatest heat loss and the subsequent density anomaly patterns induced by the NAO (Figure 3). While positive density changes are largest near the Irminger Sea region, the strongest heat losses are found in the Labrador Sea (strongest in its western part).

The fact that wind stress curl variability, and associated heat losses in the Labrador Sea, lead changes in Irminger Sea density by about 1 year, Figure 3, suggests a role for advection of waters from the Labrador Sea toward the Irminger Sea by the gyre circulation. To investigate this potential mechanism, we perform a backward Lagrangian analysis based on altimetry-derived geostrophic velocities to identify the origin of water, that is, the simulated Lagrangian trajectories (Figure 4), reaching the Irminger Sea as well as the Iceland Basin.

Figure 4 shows that the origin of water reaching the Irminger Sea (Figure 4a) versus the Iceland Basin (Figure 4b) from the Labrador Sea differs in key ways. Particles arriving at the Iceland Basin and originating in the Labrador Current (similar to what has been put forward by Holliday et al. (2020)), trace the zone between the closed dynamic height contours of the subpolar gyre and the open contours connecting to the Nordic Seas. The particles are concentrated in the gyre boundary currents throughout their advective path. In contrast, the particles arriving in the Irminger Sea from the Labrador Sea have spread into the gyre interior and have stayed within the closed mean dynamic height contours. This provides observational evidence of advective pathways directly linking the Labrador Sea with the Irminger Sea via the interior of the gyre. Based on a histogram of the particle ages, the median transit time for these particles traced from the Irminger Sea toward the Labrador Sea is about 2 years but start entering this region already after a few months (see Figure S3 in Supporting Information S1 for more details about the transit times of all experiments in Figure 4). The longer timescale derived from the altimetry-derived surface velocity product is a direct result of the smoothing inherent in the product's absolute velocity field.

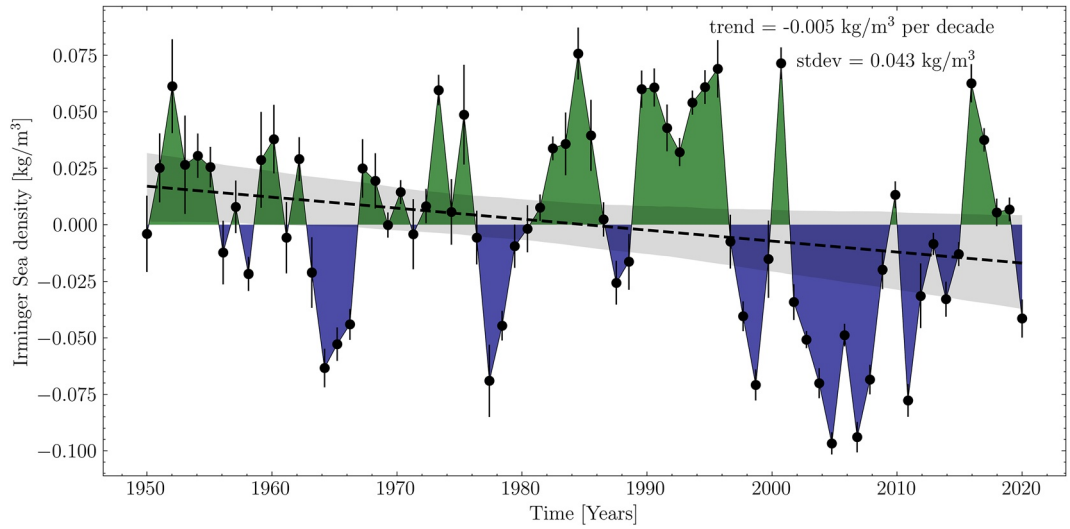

Figure 5. Long-term changes of annual-mean Irminger Sea density anomalies (cf. box as in Figure 1d) for the 1950–2019 period. The annual cycle is removed before the analysis. The standard error is shown by the bars and the standard deviation (stdev) is also given. The trend line is shown in dashed black and the gray shading denotes the 95% confidence intervals. The slope of the trend line is −0.005 kg/m^3 per decade but not significant at the 95% confidence level assessed using the modified Mann-Kendall trend test (Hamed & Rao, 1998).

Water can also reach the Irminger Sea and Iceland Basin from the subtropics via the North Atlantic Current (NAC) (Figures 4c and 4d). Backtracking particles from the Iceland Basin to the subtropics, Figure 4d, reveals that they trace the same dynamic height contours within the Iceland Basin as for the Labrador Sea-origin water (cf. Figure 4b) but are more concentrated along the central branch of the NAC (higher particle density). This is different from the subtropical-origin Irminger Sea particles (Figure 4c), which arrive via a "short-cut" from the northern branch of the NAC that separates from the main NAC just east of the mid-Atlantic ridge (e.g., Daniault et al., 2016). The subtropical-origin water stays mainly in the boundary currents, and most importantly, these trajectories communicate minimally and only occasionally (possibly through eddy stirring) with the interior Irminger Basin (Figure 4c). This result provides evidence that water from the interior of the Labrador Sea spreads into the interior Irminger Sea where it is further transformed as part of the subpolar AMOC (Petit et al., 2020). It highlights the distinction between origins and pathways of the boundary currents versus the interior of the basins, and therefore the different evolution of density anomalies.

3.4. What Can Irminger Sea Density Tell us About the Strength of the Subpolar AMOC Over the Last 70 Years?

There is evidence in the literature that proxies or fingerprints that explain a specific AMOC timescale or mechanism are not necessarily reliable indicators or predictors of long-term AMOC change (e.g., Little et al., 2020; Jackson & Wood, 2020), and that there may be alternative explanations for density variability that are unrelated to the overturning (e.g., L. Li et al., 2022). However, the strong relationship between Irminger Sea density and subpolar AMOC change present in OSNAP and GloSea5 provides us with a robust, albeit indirect, measure that can be used to examine long-term AMOC trends.

In Figure 5, we examine the long-term annual-mean density anomalies (annual cycle removed) in the SPNA with focus on the Irminger Sea. The Irminger Sea density time series shows a multi-year variability with positive and negative density anomalies during the 1970–1990 and 1996–2010 period, respectively. The long-term change of this time series over the past 70 years is −0.035 kg/m^3 (or −0.005 kg/m^3 per decade). Using the observed regression slope between Irminger Sea density and AMOC at OSNAP East (Figure 1c), this decline implies a weakening of ∼2.2 Sv or 13% over this period, which is not inconsistent with the Caesar et al. (2018) estimate of 3 ± 1 Sv since the mid-twentieth century. However, because of the large interannual and decadal variability seen in Figure 5, this linear trend remains statistically insignificant at the 95% confidence level.

To provide some basin-wide context to our result, we now discuss recent studies that have reconstructed the MOC in the North Atlantic. Recently, Fraser and Cunningham (2021) used a Bernoulli inverse applied to hydrography to reconstruct the AMOC at 50°N and concluded that no significant AMOC weakening trend over the past 120 years was found in the SPNA. Rossby et al. (2020) used hydrographic casts to reconstruct the dynamic height difference north and south of the Greenland-Scotland Ridge to estimate the strength of the warm water inflow into the Nordic Seas and concluded that this upper branch of the MOC remains stable with no evident long-term increase or decrease. This is in agreement with Orvik (2022), who found no evidence for change in volume or heat transport in the shorter (1995–2020) but directly measured time series of currents and temperatures in the core of the Norwegian Atlantic Current. A similar stability of the subtropical and subpolar AMOC since the 1990 has also been reported by Fu et al. (2020) that combined repeated hydrographic sections with an inverse model constrained using satellite altimetry. Jackson et al. (2022) concluded that there is no evidence for an AMOC slowdown both in the subtropics and the SPNA since 1980, although these authors recognize that a weakening on longer timescales such as that expected from anthropogenic warming may simply be obscured by the large interannual and decadal variability. Taken together, we conclude that there is yet no consensus regarding basin-wide North Atlantic slowdown of the overturning circulation.

4. Conclusions

The main conclusion of this study is that the Irminger Sea is herein highlighted as the center of action for subpolar AMOC variability. This finding is rooted in direct AMOC estimates from the OSNAP array (2014–2018) and supported by similar results from an ocean reanalysis (1993–2018). We further demonstrate that the subpolar AMOC at the eastern part of the OSNAP array can be reconstructed using Irminger Sea density or satellite-derived sea-surface heights, and that the NAO is the main mechanism driving Irminger Sea density variations on multiple timescales. However, we were unable to connect local atmospheric heat losses to changes in Irminger Sea densities on interannual to decadal time scales. Instead, we highlight observational evidence from a Lagrangian perspective that waters dominating the central Irminger Sea are cooled in the first place in the Labrador Sea where the largest heat losses take place as a result of strong NAO periods. The interior Labrador Sea waters are advected via the gyre circulation into the interior of the Irminger Sea, where density anomalies appear 1 year after initial cooling in the Labrador Sea.

Having established confidence in the robust connection between subpolar overturning and density variations in the Irminger Sea from both the OSNAP array and an ocean reanalysis, we use this proxy as an indicator of long-term subpolar AMOC changes. Our analysis shows a suggestive but statistically insignificant weakening of 2.2 Sv or 13% of the subpolar AMOC at its center of action over the past 70 years. Detecting a significant long-term trend is indeed complicated by the strong interannual and decadal variability at subpolar latitudes. Based on this result, and recent studies reconstructing the MOC at different latitudes, we conclude that no consensus is yet reached regarding basin-wide North Atlantic slowdown of the overturning circulation. Finally, our finding that, on decadal timescales, cold dense upper ocean is associated with strong subpolar AMOC indeed challenges the common paradigm from modern and paleo studies that cold sea-surface temperatures in the North Atlantic are associated with a weakening overturning. This general assumption thus needs to be looked at again.

Data Availability Statement

The metoffice EN4 hydrographic data can be accessed through this link: https://www.metoffice.gov.uk/hadobs/en4/download-en4-2-1.html. The DUACS DT2018 SSH data is from the Copernicus Marine Environment Monitoring Service (CMEMS) and can be accessed through this link: https://resources.marine.copernicus.eu/products. The CMEMS GloSea5 ocean reanalysis can be accessed here: https://resources.marine.copernicus.eu/product-detail/GLOBAL_REANALYSIS_PHY_001_031/INFORMATION. The NCEP/NCAR reanalysis data set can be found here: https://psl.noaa.gov/data/gridded/data.ncep.reanalysis.html. The corrected OSNAP AMOC time series can be accessed from here: https://smartech.gatech.edu/handle/1853/65537.

Acknowledgments
The authors acknowledge support by the UK Natural Environment Research Council National Capability programme CLASS (NE/R015953/1), NERC grants UK OSNAP (NE/K010875/1 and NE/K010875/2) and UK OSNAP Decade (NE/T00858X/1). The authors would like to thank the two anonymous reviewers for their constructive comments that helped to improve our manuscript. A special thanks to J. Baker and L. Jackson at the Met Office for providing the GloSea5 AMOC time series, and to E. Eisbrenner at Stockholm University for setting up the Lagrangian code.

References

Blockley, E., Martin, M., McLaren, A., Ryan, A., Waters, J., Lea, D., et al. (2014). Recent development of the met office operational ocean forecasting system: An overview and assessment of the new global foam forecasts. *Geoscientific Model Development*, *7*(6), 2613–2638. https://doi.org/10.5194/gmd-7-2613-2014

Caesar, L., Rahmstorf, S., Robinson, A., Feulner, G., & Saba, V. (2018). Observed fingerprint of a weakening Atlantic Ocean overturning circulation. *Nature*, *556*(7700), 191–196. https://doi.org/10.1038/s41586-018-0006-5

Chafik, L., & Rossby, T. (2019). Volume, heat, and freshwater divergences in the subpolar North Atlantic suggest the Nordic Seas as key to the state of the meridional overturning circulation. *Geophysical Research Letters*, *46*(9), 4799–4808. https://doi.org/10.1029/2019gl082110

Daniault, N., Mercier, H., Lherminier, P., Sarafanov, A., Falina, A., Zunino, P., et al. (2016). The Northern North Atlantic Ocean mean circulation in the early 21st century. *Progress in Oceanography*, *146*, 142–158. https://doi.org/10.1016/j.pocean.2016.06.007

Dawson, A. (2016). eofs: A library for EOF analysis of meteorological, oceanographic, and climate data. *Journal of Open Research Software*, *4*(1), 14. https://doi.org/10.5334/jors.122

Desbruyères, D., Chafik, L., & Maze, G. (2021). A shift in the ocean circulation has warmed the subpolar North Atlantic Ocean since 2016. *Communications Earth & Environment*, *2*(1), 1–9. https://doi.org/10.1038/s43247-021-00120-y

Döös, K., Jönsson, B., & Kjellsson, J. (2017). Evaluation of oceanic and atmospheric trajectory schemes in the TRACMASS trajectory model v6. 0. *Geoscientific Model Development*, *10*(4), 1733–1749. https://doi.org/10.5194/gmd-10-1733-2017

Foukal, N. P., & Lozier, M. S. (2017). Assessing variability in the size and strength of the North Atlantic subpolar gyre. *Journal of Geophysical Research: Oceans*, *122*(8), 6295–6308. https://doi.org/10.1002/2017jc012798

Frajka-Williams, E. (2015). Estimating the Atlantic overturning at 26°N using satellite altimetry and cable measurements. *Geophysical Research Letters*, *42*(9), 3458–3464. https://doi.org/10.1002/2015gl063220

Fraser, N. J., & Cunningham, S. A. (2021). 120 years of AMOC variability reconstructed from observations using the Bernoulli inverse. *Geophysical Research Letters*, *48*(18), e2021GL093893. https://doi.org/10.1029/2021gl093893

Fu, Y., Li, F., Karstensen, J., & Wang, C. (2020). A stable Atlantic meridional overturning circulation in a changing North Atlantic Ocean since the 1990s. *Science Advances*, *6*(48), eabc7836. https://doi.org/10.1126/sciadv.abc7836

Good, S. A., Martin, M. J., & Rayner, N. A. (2013). EN4: Quality controlled ocean temperature and salinity profiles and monthly objective analyses with uncertainty estimates. *Journal of Geophysical Research: Oceans*, *118*(12), 6704–6716. https://doi.org/10.1002/2013jc009067

Häkkinen, S., & Rhines, P. B. (2004). Decline of subpolar North Atlantic circulation during the 1990s. *Science*, *304*(5670), 555–559. https://doi.org/10.1126/science.1094917

Häkkinen, S., Rhines, P. B., & Worthen, D. L. (2011). Warm and saline events embedded in the meridional circulation of the northern North Atlantic. *Journal of Geophysical Research*, *116*(C3), C03006. https://doi.org/10.1029/2010jc006275

Hamed, K. H., & Rao, A. R. (1998). A modified Mann-Kendall trend test for autocorrelated data. *Journal of Hydrology*, *204*(1), 182–196. https://doi.org/10.1016/s0022-1694(97)00125-x

Holliday, N. P., Bersch, M., Berx, B., Chafik, L., Cunningham, S., Florindo-López, C., et al. (2020). Ocean circulation causes the largest freshening event for 120 years in eastern subpolar North Atlantic. *Nature Communications*, *11*(1), 585. https://doi.org/10.1038/s41467-020-14474-y

Hu, S., & Fedorov, A. V. (2020). Indian Ocean warming as a driver of the North Atlantic warming hole. *Nature Communications*, *11*(1), 1–11. https://doi.org/10.1038/s41467-020-18522-5

Jackson, L. C., Biastoch, A., Buckley, M. W., Desbruyères, D. G., Frajka-Williams, E., Moat, B., & Robson, J. (2022). The evolution of the North Atlantic meridional overturning circulation since 1980. *Nature Reviews Earth & Environment*, *3*(4), 1–14. https://doi.org/10.1038/s43017-022-00263-2

Jackson, L. C., Peterson, K. A., Roberts, C. D., & Wood, R. A. (2016). Recent slowing of Atlantic overturning circulation as a recovery from earlier strengthening. *Nature Geoscience*, *9*(7), 518–522. https://doi.org/10.1038/ngeo2715

Jackson, L. C., & Wood, R. (2020). Fingerprints for early detection of changes in the AMOC. *Journal of Climate*, *33*(16), 7027–7044. https://doi.org/10.1175/jcli-d-20-0034.1

Kalnay, E., Kanamitsu, M., Kistler, R., Collins, W., Deaven, D., Gandin, L., et al. (1996). The NCEP/NCAR 40-year reanalysis project. *Bulletin of the American Meteorological Society*, *77*(3), 437–471. https://doi.org/10.1175/1520-0477(1996)077<0437:tnyrp>2.0.co;2

Keil, P., Mauritsen, T., Jungclaus, J., Hedemann, C., Olonscheck, D., & Ghosh, R. (2020). Multiple drivers of the North Atlantic warming hole. *Nature Climate Change*, *10*(7), 667–671. https://doi.org/10.1038/s41558-020-0819-8

Li, F., Lozier, M. S., Bacon, S., Bower, A., Cunningham, S., de Jong, M., et al. (2021). Subpolar North Atlantic Western boundary density anomalies and the meridional overturning circulation. *Nature Communications*, *12*(1), 1–9. https://doi.org/10.1038/s41467-021-23350-2

Li, F., Lozier, M. S., Danabasoglu, G., Holliday, N. P., Kwon, Y.-O., Romanou, A., et al. (2019). Local and downstream relationships between Labrador Sea water volume and North Atlantic meridional overturning circulation variability. *Journal of Climate*, *32*(13), 3883–3898. https://doi.org/10.1175/jcli-d-18-0735.1

Li, L., Lozier, M. S., & Li, F. (2022). Century-long cooling trend in subpolar North Atlantic forced by atmosphere: An alternative explanation. *Climate Dynamics*, *58*(9), 2249–2267. https://doi.org/10.1007/s00382-021-06003-4

Little, C. M., Zhao, M., & Buckley, M. W. (2020). Do surface temperature indices reflect centennial-timescale trends in Atlantic meridional overturning circulation strength? *Geophysical Research Letters*, *47*(22), e2020GL090888. https://doi.org/10.1029/2020gl090888

Lozier, M. S. (2012). Overturning in the North Atlantic. *Annual Review of Marine Science*, *4*(1), 291–315. https://doi.org/10.1146/annurev-marine-120710-100740

Lozier, M. S., Bacon, S., Bower, A. S., Cunningham, S. A., De Jong, M. F., De Steur, L., et al. (2017). Overturning in the subpolar North Atlantic program: A new international ocean observing system. *Bulletin of the American Meteorological Society*, *98*(4), 737–752. https://doi.org/10.1175/bams-d-16-0057.1

Lozier, M. S., Li, F., Bacon, S., Bahr, F., Bower, A., Cunningham, S., et al. (2019). A sea change in our view of overturning in the subpolar North Atlantic. *Science*, *363*(6426), 516–521. https://doi.org/10.1126/science.aau6592

Menary, M. B., Jackson, L. C., & Lozier, M. S. (2020). Reconciling the relationship between the AMOC and Labrador Sea in OSNAP observations and climate models. *Geophysical Research Letters*, *47*(18), e2020GL089793. https://doi.org/10.1029/2020gl089793

Moat, B. I., Smeed, D. A., Frajka-Williams, E., Desbruyères, D. G., Beaulieu, C., Johns, W. E., et al. (2020). Pending recovery in the strength of the meridional overturning circulation at 26 n. *Ocean Science*, *16*(4), 863–874. https://doi.org/10.5194/os-16-863-2020

Mulet, S., Rio, M.-H., Etienne, H., Artana, C., Cancet, M., Dibarboure, G., et al. (2021). The new CNES-CLS18 global mean dynamic topography. *Ocean Science*, *17*(3), 789–808. https://doi.org/10.5194/os-17-789-2021

Orvik, K. A. (2022). Long-term moored current and temperature measurements of the Atlantic inflow into the Nordic Seas in the Norwegian Atlantic current; 1995–2020. *Geophysical Research Letters*, *49*(3), e2021GL096427. https://doi.org/10.1029/2021gl096427

Petit, T., Lozier, M. S., Josey, S. A., & Cunningham, S. A. (2020). Atlantic deep water formation occurs primarily in the Iceland basin and Irminger Sea by local buoyancy forcing. *Geophysical Research Letters*, *47*(22), e2020GL091028. https://doi.org/10.1029/2020gl091028

Rossby, T., Chafik, L., & Houpert, L. (2020). What can hydrography tell us about the strength of the Nordic Seas MOC over the last 70 to 100 years? *Geophysical Research Letters*, *47*(12), e2020GL087456. https://doi.org/10.1029/2020gl087456

Zhang, R., Sutton, R., Danabasoglu, G., Kwon, Y.-O., Marsh, R., Yeager, S. G., et al. (2019). A review of the role of the Atlantic meridional overturning circulation in Atlantic multidecadal variability and associated climate impacts. *Reviews of Geophysics*, *57*(2), 316–375. https://doi.org/10.1029/2019rg000644

Zhang, R., & Thomas, M. (2021). Horizontal circulation across density surfaces contributes substantially to the long-term mean northern Atlantic meridional overturning circulation. *Communications Earth & Environment*, *2*(1), 1–12. https://doi.org/10.1038/s43247-021-00182-y

Zou, S., Lozier, M. S., Li, F., Abernathey, R., & Jackson, L. (2020). Density-compensated overturning in the Labrador Sea. *Nature Geoscience*, *13*(2), 1–6. https://doi.org/10.1038/s41561-019-0517-1